



ACOUSTICS 2012

Overview of CAA techniques applied to various propulsion and cooling systems

S. Moreau

Université de Sherbrooke, 2500 boulevard de l'université, Sherbrooke, Canada J1K2R1
stephane.smoreau@gmail.com

Noise reduction driven by more stringent specifications requires the introduction of acoustic predictions in the design process of many flow-moving machines. However, reproducing their noise spectrum especially for high-speed turbo-engines that contains both tonal and broadband components over a large range of frequencies may seem a daunting task. Two main Computational Aero-Acoustics approaches can be used to estimate noise. First, a hybrid method where the noise sources are computed accurately in a limited zone, the surface in wall-bounded cases, the shear region in free shear-layer flows and the far-field acoustic pressure is then obtained by an acoustical analogy. Secondly, direct noise computation can be performed using compressible turbulent simulations. The latter is still limited to basic flows at low Reynolds numbers, except maybe at low Mach numbers where the Lattice Boltzmann Method provides an efficient way to compute noise radiation of complex installed systems. Both paths are first illustrated on two canonical problems, airfoil self-noise and single-stream cold jet noise, and then on more complex systems such as low-speed fan noise and high-speed nozzle jet noise.

1 Introduction

Noise mitigation and reduction are becoming major drivers in our daily life. A low noise criterion is even becoming a selling argument for daily appliances such as kitchen fans, vacuum cleaners or hair dryers. The constant increase of computer power in an even smaller space requires more powerful and quieter cooling fan systems. Similarly, ventilation systems in building must meet harsher noise specifications as they are now used not only for cooling and heating needs but also for improving the air quality and removing possible undesired gases as radon. Transportation vehicles and their propulsion systems are also increasing at a constant rate and the Joint Planning and Development Office projects a three-fold increase of the density of high-altitude traffic in the United States by 2025. At the same time, the growth of major cities is catching up with the airport areas further increasing the need for quieter airplanes particularly in take-off and landing configurations. The 2020 ACARE goals set the overall noise reduction of an airplane by 10 dB compared to the level in 2000. Therefore there is an urgent need for accurate noise predictions over the whole frequency range of interest as a function of the various operating conditions and installation of a given machine and an integration of these predictions in its design and optimization process.

Unfortunately, acoustic prediction for a large frequency range is probably the most difficult task an engineer faces in the design of a product. First, a Computational Aero-Acoustics (CAA) method must provide a direct connection between the turbulent flow (yielding the high frequency range caused by the smallest turbulent eddies) and the radiated noise usually far from the source. Secondly, a CAA simulation is even more demanding than resolving the smallest eddies by a turbulent Direct Numerical Simulation (DNS) because of the disparity of scales at stake: typical acoustic velocity and pressure fluctuations are several orders of magnitude smaller than the corresponding aerodynamic ones. The earliest works on aeroacoustics are relatively recent and date back to Lighthill's pioneering work on jet in the late 1950s. They relied on dimensional analysis and acoustic analogies, which separate a source region from the propagation zone and formally solve for a wave equation with a source term including the modeled noise sources only. CAA tries to directly predict the noise sources and eventually the noise propagation. CAA is therefore much more recent and very few works have been conducted before the 2000s.

The present study is therefore a short overview of possible (CAA) methods that can be used to predict noise in various propulsion and ventilation systems (fluid machinery), and that are currently being developed and applied at the

Université de Sherbrooke (UdeS). The first two sections will focus on more canonical applications of wall-bounded and free shear layer noise. The last three will focus on more applied cases that relate to both rotating systems and complex nozzle flows. In all shown examples, both hybrid and direct noise simulations are pursued. In the former, noise sources are first computed, either at the wall or in the near-field region. A wave propagation or extrapolation is then achieved to yield the far-field acoustic pressure.

2 Canonical Noise Problems

The canonical cases of wall-bounded and free shear layer flows provide both validation cases for engineering purposes and also provide some understanding of the fundamental flow physics that leads to sound generation (the scientific goal). One example of each is given below.

2.1 Airfoil noise

One of the simplest wall-bounded noise mechanism is an airfoil self-noise, which is produced by the diffraction at the trailing edge of pressure fluctuations born in the boundary layers. To mimic aeroacoustic experiments of airfoil self-noise that currently exist at low Mach number only ($M \leq 0.2$ typically) but high Reynolds number based on the chordlength c ($Re_c \approx 1-4 \times 10^5$), the first approach consists in using more efficient incompressible flow solvers to produce the noise sources on the wall and to resort to an acoustic analogy to propagate sound to the far-field as no acoustic information is available in the flow field. Moreau *et al.* [9] showed that the flow around an airfoil in an open-jet wind tunnel facility differs significantly from that around an isolated airfoil in a uniform stream. Therefore, the computations of the noise sources are made in two steps. A 2-D Reynolds-Averaged Navier-Stokes (RANS) simulation of the complete open-jet wind tunnel configuration including the nozzle, the airfoil and most of the anechoic chamber is first achieved to capture the strong interaction between the jet and the airfoil and its impact on the airfoil load at any incidence. The $k-\omega$ SST model was found to provide the best prediction of the mean flow characteristics such as the wall pressure distribution on the airfoil and the velocity profiles at inlet or around the airfoil [9]. The full RANS simulation then provides velocity boundary conditions for a smaller Large Eddy Simulation (LES) truncated domain that is embedded in the jet potential core to avoid the resolution of the jet shear layers. For an attached flow condition, the LES computational domain typically extends 3-4 c in the streamwise x -direction,

$1-2.5 c$ in the crosswise y -direction and $\approx 0.1 c$ in the spanwise z -direction. The latter should be greatly increased when significant flow separation occurs. The grid used for such applications are regular hexahedral meshes with 2-12 million points achieving maximum values of $\Delta x^+ \approx 30 - 40$, $\Delta y^+ \approx 1$ and $\Delta z^+ \approx 20 - 30$, which meet LES requirements. All incompressible flow solvers used (Fluent, CFX, Star-CD, OpenFoam, CDP, Wang's code) were second-order accurate both in space and time. The LES sub-grid scale (SGS) model is the Dynamic Smagorinsky model. Flow statistics needed for the propagation to the far-field are typically collected over 6-10 flow-through times. For the acoustic predictions, the extension of two acoustic analogies, Amiet's and Ffowcs-Williams and Hall's models [6, 1], to finite-chord Green's functions have been used [11, 17]. This hybrid method has been successfully applied to several airfoils by various research groups: Blake's slanted plate [16], a Controlled-Diffusion (CD) airfoil [17, 4], the NACA 6512-63 [18] A typical result achieved on the CD airfoil at 8 and 15° incidence is shown in Fig. 1. The flow topology is very different for both incidences: at 8° a small recirculation bubble exists close to the leading edge and the turbulent eddies only develop close to the trailing edge; at 15°, a large flow separation starts close to the leading edge with still some small structures grazing on the suction side toward the trailing edge. Excellent agreement is reached on the wall pressure fluctuations for all simulations with a better roll-off at high frequencies for the most recent simulations. For the far-field noise prediction, the Openfoam noise sources on the finer grid is used with three different acoustic analogies. All results are similar between 400 and 1000 Hz. Beyond, Curle's analogy that assumes a compact source yields unrealistic levels. The decay is also different between the extended Amiet's and Ffowcs-Williams and Hall's analogies.

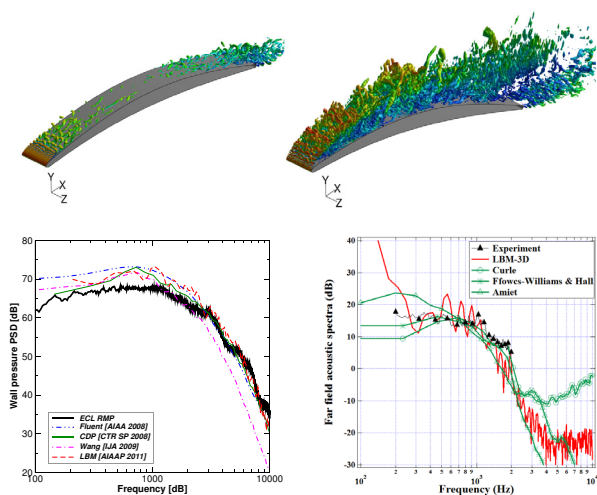


Figure 1: Self-noise of the CD airfoil in the Ecole Centrale de Lyon (ECL) wind tunnel – (top) Iso-contours of the Q -factor at 8 and 15° - (bottom left) Wall pressure spectrum close to the trailing edge at 8° - (bottom right) Far-field acoustic pressure spectrum at 8° and 90°

The second approach consists in computing the noise directly and using compressible flow solvers. Recently Sandberg *et al.* simulated several flow conditions and angles of attack on a NACA0012 airfoil [12] but at lower Reynolds numbers ($Re_c \approx 10^4$) and in free field. Extension to higher Reynolds number are currently investigated by Winkler *et*

al. [19] on the NACA 6512-63 including the more realistic non-uniform flow condition in the jet potential core of the Siegen test facility. To keep a reasonable computational time the Mach number has been increased to 0.25 after checking that the flow topology was not changing significantly in RANS $k-\omega$ SST simulations up to 0.3. An elegant alternative to classical Navier-Stokes flow solvers is Lattice-Boltzmann Method (LBM) flow solvers that look for the solutions of the discrete Boltzmann equations instead, and that can be shown to be equivalent to the compressible Navier-Stokes equations at low Mach number [3]. To be able to apply realistic boundary conditions the computational domain is now extended to most of the anechoic wind tunnel with a similar spanwise extent as the above incompressible LES to properly capture the spanwise coherence length. The large grid used in this case consists of cubic voxels with 10 refinement levels yielding about 640 million points achieving maximum values of $\Delta x^+ = \Delta y^+ = \Delta z^+ \approx 1$. To achieve the DNS resolution close to the airfoil, the Mach number has again been increased to 0.2. The simulation with Powerflow 4.3c has been run for 10 through-flow times [14]. The resulting acoustic field described by the instantaneous dilatation field is shown in Fig. 2. The trailing-edge noise radiation is clearly seen with a distorted cardioid shape caused by the nozzle-lip diffraction. Some high-frequency noise is also produced at the re-attachment point of the recirculation bubble at the leading edge. The wall pressure fluctuations close to the trailing edge shown in Fig. 2 (bottom left) match very well with experiment and the direct noise calculation shown in Fig. 2 (bottom left) also. When comparing with the hybrid methods, the direct noise simulation suggests that the results obtained with Ffowcs-Williams and Hall's analogy are more accurate at high frequencies.

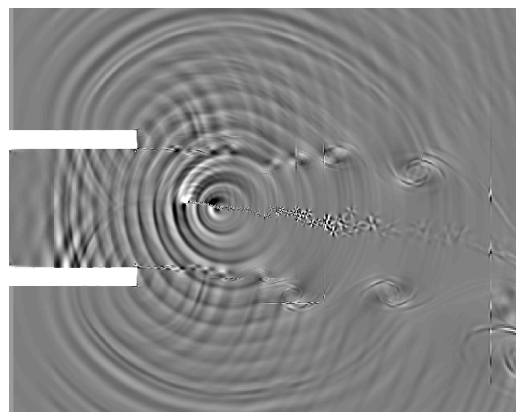


Figure 2: Instantaneous dilatation field in the large anechoic chamber at Ecole Centrale de Lyon.

2.2 Canonical single-stream cold jet

One of the simplest free shear-layer noise mechanism is the noise produced by a single-stream cold jet. Several experimental and numerical studies have been achieved on the canonical jet at the Mach number based on the jet exit velocity U_j , $M_j=0.9$ and a Reynolds number based on the jet diameter D , $Re_D=4 \cdot 10^5$. Most of numerical studies involved high-order compact schemes (sixth to thirteenth order spatial discretization) on structured cartesian grids (see for instance [2] and the references therein). In order to be able to tackle more complex nozzle geometries with chevrons, tabs and poten-

tially multiple streams and lobe-mixers, the present approach pursued at UdeS involve lower-order schemes on unstructured grids. The latter are finite-element Taylor-Galerkin or Galerkin schemes [5] as implemented in the AVBP code jointly developed by Cerfacs and IFP [15]. Non-reflecting boundary conditions are imposed to prevent reflections at the boundaries of the computational domain. A sponge layer is added to damp the vortices and perturbations to prevent spurious effects on inlet and outlet boundary conditions. The computational domain is a rectangular box 40 diameters long in the streamwise jet direction (x), and from $-15 D$ to $15 D$ wide in the transverse directions. The mesh consists of about 10-100 million tetrahedral elements (≈ 2 -20 million nodes), with a first slight (4%) increase of the spacing in the streamwise direction and an exponential coarsening for the final part ($x > 25D$). The grid is exponentially stretched from the lip-line to the transverse boundaries. To ensure a good symmetry of the node distribution, the grid is generated on a fourth of the computational domain and duplicated by rotation around the jet axis. The main jet stream is initialized through a classical tangential velocity profile and an inlet temperature profile adopted from Crocco-Buseman relation, assuming constant pressure [2]. A random forcing is required to destabilize the initial cylindrical laminar jet. Small random velocity disturbances in the form of 10 azimuthal modes with random amplitudes scaled by 1% of U_j (vortex ring excitation) are added to the instantaneous field in the shear layer of the jet as suggested by Bogey and Bailly [2]. Whereas Bogey and Bailly uses a high-order explicit filtering, a classical explicit SGS viscosity is applied here within the filtered equation system using either the WALE or the Dynamic Smagorinsky model. No significant differences are found between the two models. Finally the far-field sound prediction is computed with the McGill Acoustic Analogy Package (MCAAP) that uses a modified porous Ffowcs Williams-Hawkings (FWH) acoustic analogy termed Formulation 1C [10].

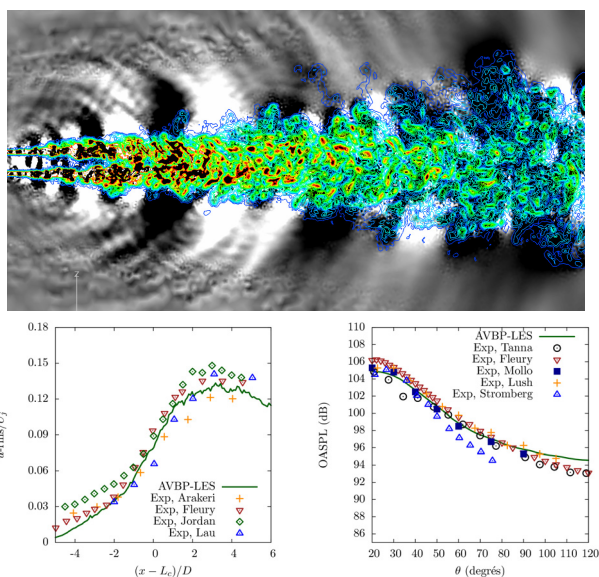


Figure 3: Single-stream cold jet ($M_j=0.9$ and $Re_D=4 \cdot 10^5$) (top) Iso-contours of the instantaneous pressure field and vorticity - (bottom left) Fluctuations of streamwise velocity on the jet centerline - (bottom right) Far-field Overall Sound Pressure Level (OASPL) at $100 D$.

A typical result achieved with the Two-steps Taylor-Galerkin scheme TTG4A on this canonical jet is shown in Fig. 3. The iso-contours of the instantaneous dilation field and vorticity clearly show the proper development of turbulence in the jet and the correct potential core length, and consequently a noise radiation with two main components: a low-frequency component at 30° (collapse of larger coherent structures at the end of the potential core) and a mid- and high-frequency component at 90° (turbulent mixing). The bottom plots confirm that both the noise sources (velocity fluctuations) and the far-field acoustic radiation are correctly predicted compared to the available experimental data. When the perturbation is too small, too weak or not correctly discretized, the OASPL shows some excessive noise at a Strouhal number of about 0.4 caused by the classical vortex pairing of the destabilizing laminar shear layer yielding an additional noise source radiating in all directions and yielding an overall increase of the OASPL by about 10 dB. It was also found that a significant improvement is achieved when third-order schemes are used compared to second-order one. Moreover the Two-steps Taylor-Galerkin scheme TTGC and the Galerkin/Runge-Kutta (GRK3) finite-element schemes are not enough dissipative at high frequencies and may lead to spurious noise radiation mainly at 90° of the jet axis.

3 More Realistic Noise Problems

The next step is to apply the above hybrid and direct noise calculation to more applied cases that relate to both rotating systems and complex nozzle flows.

3.1 Low-speed Rotating Machines

The first application is representative of low-speed ventilation fan systems for which the tip Mach number is far less than 0.3. Installed on a support in a system, these machines radiate both tonal and broadband noise with often similar amplitudes at design conditions. The former will increase at high flow rates and the former at low flow rates when the fan approaches stalls. Tonal noise predictions can be successfully predicted by Unsteady RANS (U-RANS) $k-\omega$ SST simulations [8, 13]. It was also shown that reconstructed wall pressure and velocity statistics from the simulated averaged flow field could yield adequate noise sources that, coupled with some of the above acoustic analogies, would yield the high frequency range of such axial and radial fan systems. Yet, the low- and mid-frequency broadband range was largely underpredicted, especially sub-harmonic broadband humps that can be seen in the experimental power spectrum shown in Figs. 4 and 5. This spectrum was obtained on a typical automotive engine cooling in a reverberant tunnel where the fan is flush-mounted on a plenum and exhausts into the reverberant room. This configuration can be first simulated with an incompressible flow solver to yield the noise sources on the blade surface that are then fed to an acoustic analogy. Fig. 4 shows the results obtained with CFX-13 using the U-RANS SAS model. The latter adjusts the turbulence length scale to the local flow inhomogeneities using the local generalized von Karman length scale, such that a large range of turbulent structures are captured. These turbulent vortices are clearly seen in the iso-contours of the Q -factor, especially the large coherent structures that wrap around the

rotating ring and that periodically chopped by the faster spinning blades. The overall performances are well predicted as illustrated by the pressure rise as a function of volumic flow rate. The sound power spectrum is also nicely recovered on the finer grid and noticeably the sub-harmonic humps caused by the above large vortical structures.

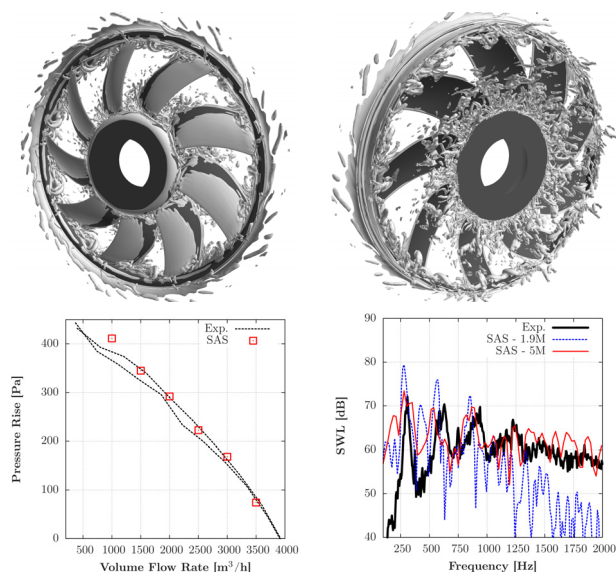


Figure 4: SAS results on an engine cooling fan at design condition – (top) Iso-contours of the Q -factor - (bottom left) Overall pressure rise as a function of flow rate - (bottom right) Far-field acoustic sound power spectrum.

Another approach is again to compute the noise directly by a compressible flow solver. The compressible Navier-Stokes flow solver Turb'flow jointly developed by ECL and Fluorem was shown to capture the humps correctly at the same frequency as the above SAS results, but could not yield the broadband level between them. An alternative way is again to use a LBM solver. Fig. 5 shows the results obtained with Powerflow 4.3c using the VLES model. Fine turbulent structures are again captured and the overall performances well predicted. With a 0.5 mm minimum voxel size, grid convergence is achieved even on the sound power spectrum that again clearly shows the sub-harmonic humps at the same frequencies as the other unsteady simulations.

3.2 High-Speed Turbo-Engines

Similarly to low-speed fans, the tonal content of high-speed turbo-engines can be predicted by U-RANS simulations to yield the noise sources on the blades. The acoustic pressure could then be propagated by an acoustic analogy in an annular duct to reproduce the complex modal content in this ducted configuration especially at high frequency [7] or by a Linearized Euler Equations solver to account for mean speed variations. Computing the actual broadband noise component is even more challenging, and can only be envisioned for a single high-pressure turbine stator vane for which Re_c is about 10^5 .

At the exhaust of a turbo-engine, the jet noise produced by the actual nozzle can be predicted with the method exposed above. Single jet simulations have been achieved on two different NASA nozzles: the ARN2 and the SMC00. Fig. 6 shows the results for the above flow conditions in the latter nozzle. The same meshing strategy is used here with

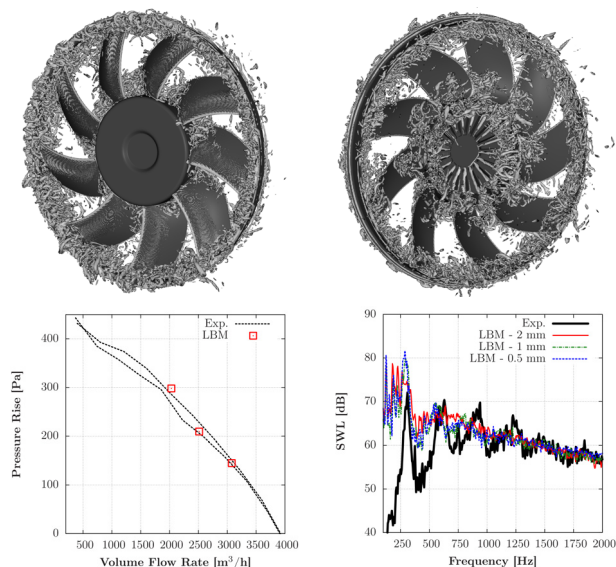


Figure 5: LBM results on an engine cooling fan at design condition – (top) Iso-contours of the Λ_2 -factor - (bottom left) Overall pressure rise as a function of flow rate - (bottom right) Far-field acoustic sound power spectrum.

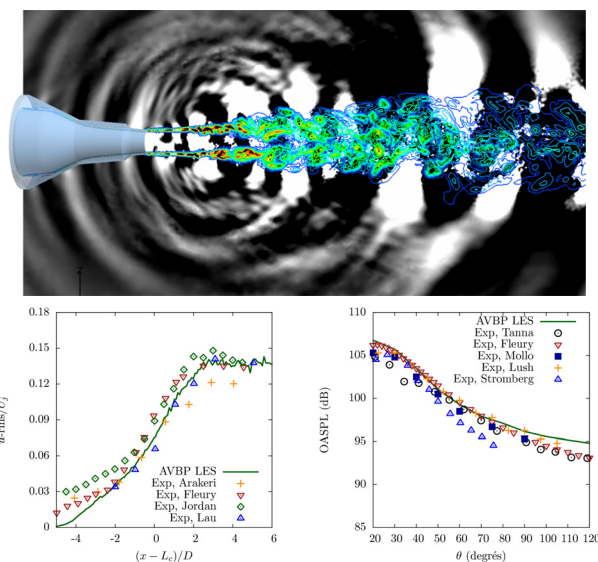


Figure 6: Cold jet with nozzle ($M_j=0.9$ and $Re_D=4 \cdot 10^5$) (top) Iso-contours of the instantaneous dilation field and vorticity - (bottom left) Fluctuations of streamwise velocity on the jet centerline - (bottom right) Far-field Overall Sound Pressure Level (OASPL) at $100 D$.

the refined zone starting in the nozzle and concentrated in the noise source region. Nevertheless some forcing as described before is still required within the nozzle to prevent laminar vortex pairing at the nozzle exit. The prediction of the velocity fluctuations on the jet centerline (similar results on the lip line) and the OASPL at $100 D$ in the bottom figures are as good as for the above canonical case even for a relatively coarse grid of 4.5 million nodes and 26 million elements. The achieved spectral resolution on this mesh is up to a Strouhal number based on D and U_j of 2. Good flow similarity is also found in the turbulent regions. Simulations on a co-axial dual stream jet are also on-going on a grid with 60 million elements. Aerodynamic results are already showing good agreement with the corresponding experimental data.

4 Conclusion

A short overview of CAA methods have been presented that can help understand acoustic sources, which could then lead to significant noise reduction to meet future noise specifications. They can be classified into hybrid methods on the one hand, where the noise sources are first computed and then used in an acoustic analogy for noise generation and propagation in the far-field, and into direct noise computations with compressible flow solvers on the other hand. They have been first applied to two canonical problems of wall-bounded and free shear layer flows. For airfoil noise, both approaches have yielded good noise prediction, the direct noise computation helping validating the most accurate acoustic analogy, and providing some hints on possible additional noise sources besides pure trailing-edge noise. For the single-stream jet noise, the Taylor-Galerkin schemes have been shown to yield accurate results provided the same forcing and the same shear-layer thickness are imposed at the inlet as with higher-order compact schemes on structured cartesian grid. The two methods have then been applied to more complex industrial cases, a low-speed engine cooling fan and a high-speed nozzle jet respectively. In the former both methods have provided insight on some rotational instability that occurs in the tip clearance and that causes narrow-band humps. In the latter similar good aerodynamic and acoustical results have been obtained as for the canonical case. At low Mach number, alternative methods to classical Navier-Stokes solvers such as LBM can handle complex systems more easily and predict noise levels within a reasonable time provided high power computing resources are available.

Acknowledgments

This research has been supported by several grants from the Natural Sciences and Engineering Research Council of Canada and the necessary computational resources have been provided by the RQCHP (Quebec) and Compute Canada.

References

- [1] R. K. Amiet. Noise due to turbulent flow past a trailing edge. *J. Sound Vib.*, 47(3):387–393, 1976.
- [2] C. Bogey and C. Bailly. Turbulence and energy budget in a self-preserving round jet: direct evaluation using large eddy simulation. *J. Fluid Mech.*, 627:129–160, 2009.
- [3] H. Chen. Volumetric formulation of the lattice boltzmann method for fluid dynamics: Basic concept. *Phys. Rev. E*, 58(3):3955–3963, September 1998.
- [4] J. Christophe, J. Anthoine, and S. Moreau. Trailing edge noise of a controlled-diffusion airfoil at moderate and high angle of attack. In *15th AIAA/CEAS Aeroacoustics Conference*, AIAA Paper 2009–3196, May 2009.
- [5] O. Colin and M. Rudgyard. Development of high-order taylor-galerkin schemes for unsteady calculations. *J. Comp. Phys.*, 162(2):338–371, 2000.
- [6] J. E. Ffowcs Williams and L. H. Hall. Aerodynamic sound generation by turbulent flow in the vicinity of a scattering half plane. *J. Fluid Mech.*, 40:657–670, 1970.
- [7] M. E. Goldstein. *Aeroacoustics*. McGraw-Hill, New York, 1976.
- [8] S. Moreau, M. Henner, D. Casalino, J. Gullbrand, G. Iaccarino, and M. Wang. Toward the prediction of low-speed fan noise. In *Proc. 2006 Summer Prog. Center for Turbulence Research, Stanford Univ./NASA Ames*, 2006.
- [9] S. Moreau, M. Henner, G. Iaccarino, M. Wang, and M. Roger. Analysis of flow conditions in freejet experiments for studying airfoil self-noise. *AIAA J.*, 41(10):1895–1905, 2003.
- [10] A. Najafi-Yazdi, G. A. Brès, and L. Mongeau. An acoustic analogy formulation for moving sources in uniformly moving media. *Philos. Trans. Royal Soc. London. Series A*, 467(2125):144–165, March 2011.
- [11] M. Roger and S. Moreau. Back-scattering correction and further extensions of amiet’s trailing edge noise model. part 1: theory. *J. Sound Vib.*, 286 (3):477–506, 2005.
- [12] R.D. Sandberg, L.E. Jones, N.D. Sandham, and P.F. Joseph. Direct numerical simulations of tonal noise generated by laminar flow past airfoils. *J. Sound Vib.*, 320(4-5):838–858, 2009.
- [13] M. Sanjose and S. Moreau. Unsteady numerical simulations of a low-speed radial fan for aeroacoustics predictions. In *ISROMAC-14, Acoustics*, Honolulu, HI, February 2012.
- [14] M. Sanjose, S. Moreau, A. Najafi-Yazdi, and A. Fosso-Pouangue. A comparison between galerkin and compact schemes for jet noise simulations. In *17th AIAA/CEAS Aeroacoustics Conference*, AIAA2011–2833 paper, June 2011.
- [15] T. Schönfeld and M. Rudgyard. Steady and unsteady flows simulations using the hybrid flow solver avbp. *AIAA J.*, 37(11):1378–1385, 1999.
- [16] M. Wang and P. Moin. Computation of trailing-edge flow and noise using large-eddy simulation. *AIAA J.*, 38(12):2201–2209, 2000.
- [17] M. Wang, S. Moreau, G. Iaccarino, and M. Roger. Les prediction of wall-pressure fluctuations and noise of a low-speed airfoil. *Int. J. Aeroacoust.*, 8(3):177–197, 2009.
- [18] J. Winkler, T. Carolus, and S. Moreau. Airfoil Trailing-Edge Blowing: Broadband Noise Prediction from Large-Eddy Simulation. In *15th AIAA/CEAS Aeroacoustics Conference*, AIAA2009–3200 paper, Miami, United-States, May 2009.
- [19] J. Winkler, R.D. Sandberg, and S. Moreau. Direct numerical simulation of the self-noise radiated by an airfoil in a narrow stream. In *18th AIAA/CEAS Aeroacoustics Conference*, AIAA2012–XXXX paper, June 2012.